Inorg. Chem. **2008**, *47*, 9706−9715

Inorganic Chemistry
Article

Organocadmium Aminoalcoholates: Synthesis, Structure, and Materials Chemistry

Andrew L. Johnson, Nathan Hollingsworth, Gabriele Kociok-Köhn, and Kieran C. Molloy*

Department of Chemistry, University of Bath, Claverton Down, Bath BA2 7AY, U.K.

Received May 16, 2008

The novel methylcadmium aminoalkoxides MeCd(dmae) (Hdmae = dimethylaminoethanol), MeCd(bdmap) [Hbdmap = 1,3-*bis*-(dimethylamino)-propan-2-ol], and MeCd(tdmap) [tdmap = 1,3-*bis*(dimethylamino)-2-(dimethylaminomethyl)-propan-2-ol] have been synthesized and structurally characterized. MeCd(dmae) (**1**) forms a tetrameric heterocubane with a Cd_4O_4 core, while MeCd(bdmap) (**2**) is trimeric and MeCd(tdmap) (**3**) is a dimer. Only in the case of MeCd(dmae) are all the ligand donors fully utilized. In solution, MeCd(tdmap) undergoes a Schlenk equilibrium, with Me_2Cd and $Cd(tdmap)_2$ evident at 218 K. The structure and solution-state chemistry of $Cd(tdmap)_2$ (**5**) have been independently studied and, in the solid-state, found to exist as a dimer whose coordination number at cadmium (CN = 6) is greater than in the organocadmium complexes (CN = 4, 5). MeCd(tdmap) has been used as a single-source precursor for CdO films by LPCVD with a glass substrate temperature of only 140 °C. Evidence is also presented for the formation of a heterometallic precursor, $[(MeZn)(MeCd)(tdmap)_2]$ (**6**), which has been used to deposit films of CdO mixed with ZnO by LPCVD at 140 °C. The structure of $Me_4Cd_4(tdmap)_2Cl_2$ (**4**), obtained serendipitously, is also included. Crystal data: **1**, $C_{20}H_{52}Cd_4N_4O_4$, FW 862.26, triclinic, $P\bar{1}$, $a = 11.47560(10)$, $b = 13.55400(10)$, $c = 21.5966(2)$ Å, $\alpha = 99.7869(4)$, $\beta = 90.7476(4)$, $\gamma = 98.7823(4)°$, $V = 3268.82(5)$ Å^3, $Z = 4$; **2**, $C_{27}H_{67}Cd_3N_6O_3$, FW 861.07, triclinic, $P\bar{1}$, $a = 11.4148(2)$, $b = 13.1886(2)$, $c = 14.3139(3)$ A, $\alpha = 102.1962(10)$, $\beta = 108.3064(10)$, $\gamma = 100.8446(10)°$, $V = 1923.09(6)$ Å^3, $Z = 4$; **3**, $C_{22}H_{54}Cd_2N_6O_2$, FW 659.51, monoclinic, $P2_1/n$, $a = 10.2912(1)$, $b = 13.46930(1)$, $c = 11.79130(1)$ Å, $\beta = 112.8051(1)°$, $V = 1506.59(2)$ Å^3, $Z = 2$; **4**, $C_{24}H_{60}Cd_4Cl_2N_6O_2$, FW 985.28, monoclinic, $P2_1/c$, $a = 10.89780(10)$, $b = 20.3529(2)$, $c = 16.5317(2)$ Å, $\beta = 94.8550(10)°$, $V = 3653.61(7)$ Å^3, $Z = 4$; **5**, $C_{40}H_{96}Cd_2N_{12}O_4$, FW 1034.09, orthorhombic, $P2_1cn$, $a = 12.33290(10)$, $b = 14.25060(10)$, $c = 29.9003(2)$ Å, $V = 5255.01(7)$ Å^3, $Z = 4$.

Introduction

Since Badeker first coated CdO upon the back of a glow discharge tube in 1907[1] CdO-based transparent conducting oxides (TCOs) have found use in a broad array of applications, including photovoltaic (PV) cells,[2] flat panel displays, and light emitting diodes.[3] As such, these films have been subject to intense investigation, both in academia and industry. Face-centered cubic cadmium oxide has a relatively low intrinsic band gap of 2.28 eV,[4] while its low effective carrier mass allows for heavily doped samples, which can have band gaps as high as 3.35 eV;[5] Sn-doped CdO can give rise to mobilities of 607 cm^2 V^{-1} s^{-1}.[6]

CdO-based TCOs have been deposited by spray pyrolysis,[7,8] reactive sputtering,[4,8,9] closed space sublimation,[10] pulsed laser deposition,[11] sol−gel[12] and electron beam

---

* To whom correspondence should be addressed. E-mail: k.c.molloy@bath.ac.uk. Tel: 00 44 1225 386382. Fax: 00 44 1225 386231.

(1) Badeker, K. *Ann. Phys.* **1907**, *22*, 748.

(2) Mathew, G. W. T. X.; Singh, V. P.; McClure, J. C.; Velumani, S.; Mathews, N. R.; Sebastian, P. J. *Sol. Energy Mater.* **2003**, *76*, 293.

(3) Yang, Q. H. Y.; Metz, A. W.; Jin, S.; Ni, J.; Wang, L.; Marks, T. J. *J. Soc. Inform. Disp.* **2005**, *13*, 383.

(4) Ueda, H. M. N.; Hosono, H.; Kawazoe, H. *J. Appl. Phys.* **1998**, *84*, 6174.

(5) Zhao, D. L. M. Z.; Ferekides, C. S. *Thin Solid Films* **2002**, *413*, 203.

(6) Yan, M. L. M.; Kannewurf, C. R.; Chang, R. P. H. *Appl. Phys. Lett.* **2001**, *78*, 234.

(7) Vigil, L. V. O.; Cruz, F.; Santana, G.; Morales-Acevedo, A.; Contreras-Puente, G. *Thin Solid Films* **2000**, 53.

(8) Frerro, R.; Rodriguez, A. J. *Sol. Energy Mater.* **2000**, *64*, 363.

(9) Subramanyam, T. K.; Srinivasulu Naidu, B.; Uthanna, S. *Appl. Surf. Sci.* **2001**, *169−170*, 529.

(10) Ferekides, D. M. C.; Viswanathan, V.; Tetali, B.; Palekis, V.; Selvaraj, P.; Morel, D. *Thin Solid Films* **2000**, *520*, 361.

(11) Ismail, R. A.; Rasheed, B. G.; Salm, E. T.; M.; Al-Hadethy, M. *J. Mater. Sci.* **2007**, *18*, 1027.

(12) Santos-Cruz, G. T.-D. J.; Castanedo-Perez, R.; Zuniga-Romero, C. I.; Zelaya-Angel, O. *Thin Solid Films* **2007**, *515*, 5381.

10.1021/ic800897t CCC: $40.75

evaporation[13] techniques, while more recently chemical vapor deposition (CVD) methods have been successfully employed. CVD is particularly attractive for TCO synthesis because of its use in conformal, large volume, thin film manufacturing processes. A key prerequisite for CVD is a volatile precursor and at present only a limited number of examples are available. Historically, CdO films have been grown via CVD using the highly toxic dimethylcadmium as a precursor;[14] however, this also requires an oxygen source such as *n*-butanol.[15] The high toxicity, moisture sensitivity, and propensity to prereaction makes dimethylcadmium a less than ideal precursor choice. The issues of using dimethylcadmium have been circumvented by the use of adducts of cadmium 1,1,1,5,5,5,-hexafluoro-2,4-pentanedionate, $Cd(hfac)_2(L)_x$, where (L) has been varied from water ($x = 2$),[16] monoglyme,[17] *N*,*N*,*N*′,*N*′-tetramethylethylenediamine (TMEDA)[14,18] and diamine derivatives thereof (all $x = 1$).[19] While $Cd(hfac)_2$ is itself polymeric in the solid-state[20] and hence of low volatility, the above adducts saturate the coordination sphere of the metal, enhance volatility, and are, to date, the most attractive precursors for CdO, albeit that they require O_2 for film deposition.

The dual-source approach of using R_2Cd and R′OH leads, naturally, to speculation as to the likelihood of organocadmium alkoxides as intermediates in this process, and thus such species would be potential single-source precursors (SSP) in their own right. While a number of simple RCdOR′ compounds have been reported (R = Me, Et; R′ = CH_3, $CHCH_3$, Bu, CHMeEt, CH_2Ph, CMe_3)[21] only one (R = Me, R′ = Bu^t)[22] had been structurally characterized until the very recent report on three further methylcadmium analogues (R′ = Me, Et, Pr^i);[23] all four adopt the tetrameric cubane structure common with the zinc analogues.[23−30]

The use of donor-functionalized alkoxides to manipulate nuclearity (and hence volatility) in metal alkoxides is a proven methodology but has not been applied to any great extent with regard to cadmium. Reaction of $MeOCH_2CH_2OH$ (Hmoe) with $(C_6F_5)_2Cd$ in various ratios has afforded the cubane $[RCd(moe)]_4$, a vertex-sharing double cubane $[R_6Cd_7(moe)_8]$, and the cage $[R_4Cd_6(moe)_8]$ (R = C_6F_5), and in each case the aggregate is stabilized by MeO:→Cd coordination.[31] Nitrogen donors, for example, pyridine, are also reported to convert the $[RCdOR′]_4$ to dimeric $[RCdOR′.py]_2$.[32] Most recently, a methylcadmium hydroxylamine, $Cd(MeCd)_4(ONEt_2)_6$, has been structurally characterized, in which a central, octahedrally coordinated, formally $Cd(ONEt_2)_6^{4-}$ tetra-anion is surrounded by four MeCd cations, with all six hydroxylamine groups utilizing both *O*, *N*-donors as bridges.[33]

Our own interest in the exploitation of donor-functionalized alkoxides in CVD precursor chemistry has prompted us to explore reactions of Me_2Cd with **I**−**III** and report our findings herein.

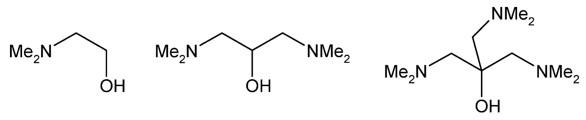

I : Hdmae **II** : Hbdmap **III**: Htdmap

Experimental Section

General Procedures. Elemental analyses were performed using an Exeter Analytical CE 440 analyzer. Room temperature ^1H, ^{13}C, and ^{113}Cd NMR spectra were recorded on either a Bruker Advance 300 or 500 MHz FT-NMR spectrometer as saturated solutions in either d^8-toluene, d^6-benzene, or $CDCl_3$, while variable temperature experiments were recorded in d^8-toluene; chemical shifts are in ppm with respect to either Me_4Si or Me_2Cd, coupling constants are in Hz. Scanning electron microscopy (SEM) was carried out on a JEOL JSM-6310 microscope equipped with Oxford Instruments ISIS EDXS attachment. X-ray diffraction (XRD) was performed using a Bruker D8 diffractometer on which coupled $\theta-2\theta$ scans were carried out. A micrOTOFQ electrospray quadrupole time-of-flight (ESI-QTOF) mass spectrometer (Bruker Daltonik GmbH, Bremen, Germany) was used to determine the molecular mass of selected compounds. This was coupled to a syringe driver (Hamilton, Bonaduz, Switzerland) and the sample dissolved in CH_2Cl_2 and infused at a rate of 3 μL/min.

Syntheses. Hdmae (**I**) was purchased from Aldrich. Hbdmap (**II**)[34] and Htdmap (**III**)[35,36] were prepared by literature methods. The preparation of **III** used a 30% excess of perbenzoic acid in chloroform at about 60 °C over a period of at least one week to achieve nearly quantitative yields. $Cd[N(SiMe_3)_2]_2$ was prepared by a modification of the literature route[37] in which $Li[N(SiMe_3)_2]$

---

(13) Mohamed, H. A.; Ali, H. M.; Mohamed, S. H.; Abd El-Raheem, M. M. *Eur. Phys. J.: Appl. Phys* **2006**, *34*, 7.

(14) Coutts, T. J.; Young, D. L.; Li, X.; Mulligan, W. P.; Wu, X. *J. Vac. Sci. Technol., A* **2000**, *18*, 2646.

(15) Irvine, S. J. C.; Ellis, D. M. *J. Mater. Sci.* **2004**, *15*, 369.

(16) Gulino, A.; Castelli, F.; Dapporto, P.; Rossi, P.; Fragala, I. *Chem. Mater.* **2002**, *14*, 704.

(17) Gulino, A.; Dapporto, P.; Rossi, P.; Fragala, I. *Chem. Mater.* **2002**, *14*, 1441.

(18) Babcock, A. W. J. R.; Mertz, A. W.; Edleman, N. L.; Metz, M. V.; Lane, M. A.; Kannewurf, C. R.; Marks, T. J. *Chem. Vap. Deposition* **2001**, *7*, 239.

(19) Ireland, J. R.; Metz, A. W.; Zheng, J.; Lobo, R. P. S. M.; Yang, Y.; Ni, J.; Stern, C. L.; Dravid, V. P.; Bontemps, N.; Kannewurk, C. R.; Poeppelmeier, K. R.; Marks, T. J. *J. Am. Chem. Soc.* **2004**, *126*, 8477.

(20) Maslen, E. N.; Greaney, T. M.; Raston, C. L.; White, A. H. *J. Chem. Soc., Dalton Trans.* **1975**, 400.

(21) Dodonov, V. A.; Pankratova, V. N.; Sorvacheva, T. M.; Nazarova, G. E. *Zh. Obshch. Khim.* **1987**, *57*, 1782.

(22) Nöth, H.; Thomann, M. *Chem. Ber.* **1995**, *128*, 923.

(23) Jana, S.; Pape, T.; Mitzel, N. W. *Z. Naturforsch.* **2007**, *62b*, 1339.

(24) Polarz, S.; Roy, A.; Merz, M.; Halm, S.; Schröder, D.; Schneider, L.; Bacher, G.; Kruis, F. E.; Driess, M. *Small* **2005**, *1*, 540.

(25) Boyle, T. J.; Bunge, S. D.; Andrews, N. L.; Matzen, L. E.; Sieg, K.; Rodriguez, M. A.; Headley, T. J. *Chem. Mater.* **2004**, *16*, 3279.

(26) Bond, A. D.; Linton, D. J.; Wheatley, A. E. H. *Acta Crystallogr., Sect. E* **2001**, *57*, m298.

(27) Driess, M.; Merz, K.; Rell, S. *Eur. J. Chem.* **2000**, 2517.

(28) Herrmann, W. A.; Bogdanovic, S.; Behm, J.; Denk, M. *J. Organomet. Chem.* **1992**, *430*, C33.

(29) Shearer, H. M. M.; Spencer, C. B. *Acta Crystallogr., Sect. B.* **1980**, *36*, 2046.

(30) Shearer, H. M. M.; Spencer, C. B. *Chem.Commun.* **1966**, 194.

(31) Busching, I.; Strasdeit, H. *Chem.Commun.* **1994**, 2789.

(32) Kennedy, J. D.; McFarlane, W. *J. Chem. Soc., Perkin Trans.* **1977**, *2*, 1187–91.

(33) Jana, S.; Fröhlich, R.; Hepp, A.; Mitzel, N. W. *Organometallics* **2008**, *27*, 1348.

(34) Campbell, K. N.; LaForge, R. A.; Campbell, B. K. *J. Org. Chem.* **1949**, *14*, 346.

(35) Müller, G.; Schätzle, T. *Z. Naturforsch., B: Chem. Sci.* **2004**, *59*, 1400.

(36) Gasteiger, J.; Herzig, C. *J. Chem. Res., Synop.* **1981**, 113.

(37) Bürger, H.; Sawodny, W.; Wannagat, U. *J. Organomet. Chem.* **1965**, *3*, 113.

Table 1. Crystallographic Data for **1**−**5**

	(**1**)	(**2**)	(**3**)	(**4**)	(**5**)
formula	$C_{20}H_{52}Cd_4N_4O_4$	$C_{27}H_{67}Cd_3N_6O_3$	$C_{22}H_{54}Cd_2N_6O_2$	$C_{24}H_{60}Cd_4Cl_2N_6O_2$	$C_{40}H_{96}Cd_2N_{12}O_4$
formula weight	862.26	861.07	659.51	985.28	1034.09
crystal system	triclinic	triclinic	monoclinic	monoclinic	orthorhombic
space group	$P\bar{1}$	$P\bar{1}$	$P2_1/n$	$P2_1/c$	$P2_1cn$
a (Å)	11.4756(1)	11.4148(2)	10.2912(1)	10.8978(1)	12.3329(1)
b (Å)	13.5540(1)	13.1886(2)	13.46930(1)	20.3529(2)	14.2506(1)
c (Å)	21.597(1)	14.3139(3)	11.79130(1)	16.5317(2)	29.9003(2)
α (deg)	99.787(1)	102.196(1)			
β (deg)	90.7476(4)	108.306(1)	112.805(1)	94.855(1)	
γ (deg)	98.782(1)	100.845(1)			
V (Å^3)	3268.82(5)	1923.09(6)	1506.59(2)	3653.61(7)	5255.01(7)
Z	4	2	2	4	4
μ(Mo-Kα) (mm^{-1})	2.593	1.675	1.438	2.471	0.856
crystal size (mm)	0.30 × 0.25 × 0.20	0.25 × 0.25 × 0.20	0.4 × 0.4 × 0.25	0.25 × 0.25 × 0.25	0.25 × 0.15 × 0.15
θ range (deg)	3.03−30.07	2.92−27.52	3.35−30.03	2.98−27.49.	2.99−27.48
refls collected	68368	30995	35529	69450	84067
independent refls	19068 [R(int) = 0.0527]	8835 [R(int) = 0.0417]	4396 [R(int) = 0.0320]	8359 [R(int) = 0.0683]	12011 [R(int) = 0.0742]
refls observed (>2σ)	13629	7325	4141	6342	9616
max, min. transmission	0.5938, 0.4846	0.7305, 0.6795	0.707, 0.587	0.537, 0.537	0.882, 0.815
R_1,[a] wR_2[b] [$I > 2\sigma(I)$]	0.0356, 0.0694	0.0319, 0.0718	0.0191, 0.0464	0.0348, 0.0714	0.0386, 0.0816
R_1,[a] wR_2 [b] (all data)	0.0648, 0.0786	0.0443, 0.0773	0.0207, 0.0474	0.0579, 0.0789	0.0595, 0.0904
goodness-of-fit[c]	1.028	1.068	1.122	1.109	1.033
largest diff. peak and hole (e Å^{-3})	0.789, −1.524	1.132, −1.182	0.624, −0.687	1.106, −1.072	0.792, −1.058
Flack parameter					−0.014(18)

[a] $R_1 = \Sigma||F_o| - |F_c||/\Sigma|F_o|$. [b] $wR_2 = \{\Sigma[w(F_o^2 - F_c^2)^2]/\Sigma[w(F_o^{2)2}]\}^{1/2}$. [c] GOF $= S = \{\Sigma[w(F_o^2 - F_c^2)^2]\ /(n - p)\}^{1/2}$.

was used in place of $Na[N(SiMe_3)_2]$. The purity of the product was verified by comparison of the ^1H and ^{13}C NMR with literature data, and by ^{113}Cd NMR (C_7H_8) [−346 ppm; lit. +641 ppm relative to 0.1 M $Cd(ClO_4)_2$ which is equivalent to −347 ppm relative to Me_2Cd].[38]

All reactions were carried out under an inert atmosphere using standard Schlenk techniques. Solvents were dried and degassed under an argon atmosphere over activated alumina columns using an Innovative Technology solvent purification system (SPS).

Synthesis of [MeCd(dmae)]$_4$ (1). Dimethylcadmium (2 mL 2.0 M solution in hexane, 4.0 mmol) was added to hexane (20 mL) and the solution cooled to −78 °C. To this mixture Hdmae (0.39 g, 4.4 mmol) was added with stirring. After 1 h the mixture was allowed to warm to room temperature whereby a white precipitate appeared which was redissolved by heating to 30 °C. Cooling in a freezer (−20 °C) gave large colorless crystals (0.65 g, 75%; mp 170 °C dec). Analysis, found (calcd for $C_5H_{13}CdNO$): C 28.1 (27.9), H 6.72 (6.08), N 6.87 (6.50)%. NMR (d^6-benzene), ^1H: 3.58 (t J = 9.8 Hz, 2H, OCH_2), 2.01 (t J = 9.8 Hz, 2H, CH_2N), 1.71 (s, 6H, NCH_3), −0.42 (s, 3H, $CdCH_3$; ^2J(^{111,113}CdH) = 72.2, 77.7 Hz). ^{13}C: 64.5 (CO), 61.0 (CH_2N), 44.8 (CH_3N), −18.2 ($CdCH_3$; ^1J(^{111,113}CdH) = 1019, 1064 Hz). ^{113}Cd: −301.

Synthesis of [MeCd(bdmap)]$_3$ (2). Dimethylcadmium (2 mL 2.0 M solution in hexane, 4.0 mmol) was added to hexane (20 mL) and the solution cooled to −78 °C. To this mixture Hbdmap (0.64 g, 4.4 mmol) was added with stirring. After 1 h the mixture was allowed to warm to room temperature whereby a white precipitate appeared which was redissolved by heating to 40 °C. Cooling in a freezer to −20 °C gave large colorless crystals (0.90 g, 83%, mp 135 °C). Analysis, found (calcd for $C_7H_{17}CdN_2O$): C 35.4 (35.2), H 7.90 (7.39), N 10.0 (10.3)%. NMR (d^6-benzene), ^1H: 3.71 (tt ^2J = 9.7 Hz, ^3J = 3.5 Hz, 1H, OCH), 1.96 (dd ^2J = 11.5 Hz, ^3J = 9.7 Hz, 2H, CH_2N), 1.86 (s, 12H, NCH_3), 1.67 (dd ^2J = 11.5 Hz, ^3J = 3.5 Hz, 2H, CH_2N), −0.51 (s, 3H, $CdCH_3$; ^2J(^{111,113}CdH) = 71.0, 73.8 Hz), ^{13}C: 67.3 (CO), 64.0 (CH_2N), 44.8 (CH_3N), −16.8 ($CdCH_3$; ^1J(^{111,113}CdH) = 1000, 1043 Hz). ^{113}Cd: −279.

Table 2. Selected Metrical Data for (**1**)[a,b]

Bond Lengths (Å)			
Cd(1)−C(1)	2.159(3)	Cd(1)−O(2)	2.238(2)
Cd(1)−N(2)	2.527(3)	Cd(1)−O(3)	2.521(2)
Cd(1)−O(1)	2.233(2)		
Bond Angles (deg)			
C(1)−Cd(1)−O(1)	130.23(10)	O(1)−Cd(1)−O(3)	84.05(7)
C(1)−Cd(1)−O(2)	149.17(11)	O(1)−Cd(1)−N(2)	100.28(8)
C(1)−Cd(1)−O(3)	102.12(11)	O(2)−Cd(1)−O(3)	74.12(7)
C(1)−Cd(1)−N(2)	100.70(12)	O(2)−Cd(1)−N(2)	73.07(8)
O(1)−Cd(1)−O(2)	80.36(7)	O(3)−Cd(1)−N(2)	145.62(8)

[a] Data for only one metal environment given for conciseness. [b] Data for only one (of two) essentially identical molecules within the asymmetric unit given.

Synthesis of [MeCd(tdmap)]$_2$ (3). Dimethylcadmium (2 mL 2.0 M solution in hexane, 4.0 mmol) was added to hexane (20 mL) and the solution cooled to −78 °C. To this mixture Htdmap (0.89 g, 4.4 mmol) was added with stirring. After 1 h the mixture was allowed to warm to room temperature whereby a white precipitate appeared which was redissolved by heating to 60 °C. Cooling to room temperature gave large colorless cube-shaped crystals (0.82 g, 62%, mp 105 °C). Analysis, found (calcd for $C_{11}H_{27}CdN_3O$): C 40.2 (40.1), H 8.70 (8.25), N 13.8 (12.7)%. NMR ($CDCl_3$), ^1H: 2.18 (s, 6H, CH_2N), 2.02 (s, 18H, CH_3N), −0.28 (s, 3H, $CdCH_3$; ^2J(^{111,113}CdH) = 73.6 Hz, unresolved). ^{13}C: 77.3 (CO), 69.2 (CH_2N), 48.6 (CH_3N), −12.2 (CH_3Cd; ^1J(^{111,113}CdC) = 1005, 960 Hz). ^{113}Cd: −228. Mass spectral data: 460.0447, calcd for [P-tdmap] 460.0451.

Synthesis of [Cd(tdmap$_2$)]$_2$ (5). *Bis*-[*bis*-(trimethylsilyl)amido]cadmium (1.59 g, 3.67mmol) was added to hexane (15 mL), the solution cooled to −78 °C and Htdmap (1.50 g, 7.35mmol) was slowly added. Stirring to room temperature gave a white precipitate and on heating to 40 °C the white precipitate dissolved giving a clear pale yellow solution. Crystals of **5** were obtained after 2 days by placing the solution in a freezer at −20 °C (1.55 g, 81%, mp 130 °C). Analysis, found (calcd for $C_{20}H_{48}\ CdN_6O_2$): C 46.2 (46.5), H 9.06 (9.36), N 16.6 (16.3) %. NMR (d^8-toluene), ^1H: 2.36 (bs CH_3N and CH_2N); ^{13}C: 69.4 (CH_2N), 48.8 (CH_3N), CO signal too weak to be observed. ^{113}Cd: −453.

---

(38) Alyea, E. C.; Fisher, K. J. *Polyhedron* **1986**, *5*, 695.

Table 3. Selected Metrical Data for (**2**)

	Bond Lengths (Å)		
Cd(1)−O(1)	2.4019(18)	Cd(3)−O(3)	2.1980(18)
Cd(1)−O(2)	2.221(2)	Cd(1)−N(4)	2.686(2)
Cd(1)−O(3)	2.2011(19)	Cd(2)−N(2)	2.489(3)
Cd(2)−O(1)	2.3417(19)	Cd(2)−N(3)	2.659(3)
Cd(2)−O(2)	2.1704(18)	Cd(3)−N(1)	2.460(3)
Cd(3)−O(1)	2.3649(19)	Cd(3)−N(5)	2.536(2)
	Bond Angles (deg)		
C(1)−Cd(1)−O(1)	114.05(11)	O(1)−Cd(2)−N(2)	72.01(7)
C(1)−Cd(1)−O(2)	128.30(13)	O(1)−Cd(2)−N(3)	139.23(7)
C(1)−Cd(1)−O(3)	129.21(13)	O(2)−Cd(2)−N(2)	108.69(8)
C(1)−Cd(1)−N(4)	98.48(13)	O(2)−Cd(2)−N(3)	71.24(7)
O(1)−Cd(1)−O(2)	73.66(7)	N(2)−Cd(2)−N(3)	96.45(8)
O(1)−Cd(1)−O(3)	77.40(6)	C(17)−Cd(3)−O(1)	110.04(11)
O(1)−Cd(1)−N(4)	140.36(7)	C(17)−Cd(3)−O(3)	154.71(11)
O(2)−Cd(1)−O(3)	102.48(8)	C(17)−Cd(3)−N(1)	105.62(12)
O(2)−Cd(1)−N(4)	68.38(7)	C(17)−Cd(3)−N(5)	100.38(12)
O(3)−Cd(1)−N(4)	99.73(8)	O(1)−Cd(3)−O(3)	78.25(6)
C(9)−Cd(2)−O(1)	120.36(12)	O(1)−Cd(3)−N(1)	72.95(8)
C(9)−Cd(2)−O(2)	143.70(12)	O(1)−Cd(3)−N(5)	149.35(7)
C(9)−Cd(2)−N(2)	107.33(13)	O(3)−Cd(3)−N(1)	99.65(8)
C(9)−Cd(2)−N(3)	100.40(12)	O(3)−Cd(3)−N(5)	72.53(7)
O(1)−Cd(2)−O(2)	75.80(7)	N(1)−Cd(3)−N(5)	102.78(8)

Synthesis of [(MeCd)(MeZn)(tdmap)$_2$] (6). Dimethylcadmium (2 mL 2.0 M solution in hexane, 4.0 mmol) and dimethylzinc (3.43 mL 1.168 M solution in toluene, 4 mmol) were added to hexane (20 mL) and the solution cooled to −78 °C. To this mixture Htdmap (1.97 mL, 8.8 mmol) was added with stirring. After 1 h the mixture was allowed to warm to room temperature whereby a white precipitate appeared which was redissolved by heating to 60 °C. Cooling to room temperature gave large colorless cube-shaped crystals (2.13 g, 87%, mp 145 °C). Analysis found (calcd for $C_{22}H_{54}CdN_6O_2Zn$): C 43.0 (43.1), H 8.94 (8.89), N 13.7 (13.7)%. NMR (d^8-toluene), ^{1}H: 2.51 (s, 12H, CH_2N), 2.31 (s, 36H, CH_3N), −0.37 (s, 3H, CH_3Cd, $^2J(^{111,113}CdH) = 746$ Hz, unresolved), −0.64 (s, 3H, CH_3Zn). ^{13}C: 78.0 (CO), 69.2 (CH_2N), 49.1 (CH_3N), −10.5 (CH_3Zn), −11.6 (CH_3Cd). ^{113}Cd: −228 and −254. Mass spectral data: 410.0717, calcd for (P-tdmap) 410.0708.

Crystal Structures. Experimental details relating to the single-crystal X-ray crystallographic studies are summarized in Table 1. For all structures, data were collected on a Nonius Kappa CCD diffracrometer at 150(2) K using Mo Kα radiation ($\lambda = 0.71073$ Å). The structures were refined using full-matrix least-squares on F^2. All non-hydrogen atoms were refined anisotropically; hydrogen atoms were included at calculated positions.

CVD Study. Films were deposited on a 76 × 26 × 1.0 mm microscope slide using a hot wall low pressure chemical vapor deposition (LPCVD) reactor which has been described in detail elsewhere.[39] A 0.15 g quantity of [MeCd(tdmap)]$_2$ (**3**) was heated to 140 °C in a tube furnace under a vacuum of about 0.1 mmHg; the glass substrate was also heated to 140 °C and the run time was 30 min. A mixed CdO/ZnO film was deposited from **6** under identical conditions.

Results and Discussion

Synthesis. The methylcadmium aminoalkoxides **1**−**3** are straightforwardly prepared from the reaction of Me_2Cd and the appropriate alcohol in 1:1 ratio. The reactions were carried out at −78 °C in hexane, then allowing the reaction mixture to warm slowly to room temperature. The solid formed was warmed to aid dissolution; crystals were obtained on cooling this mixture slowly to room temperature then at −20 °C overnight. Yields were 62−80%.

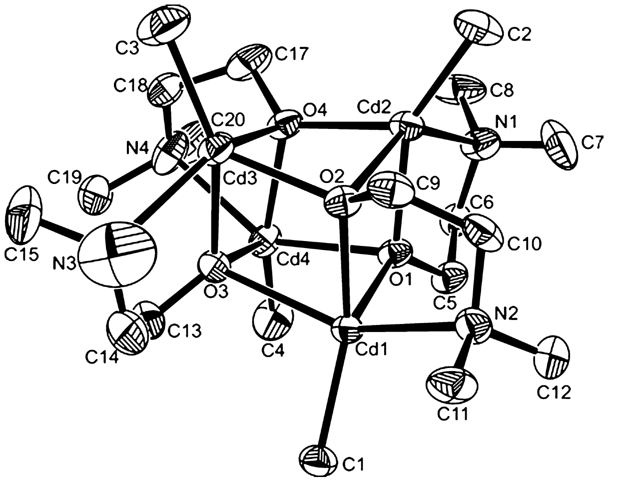

Figure 1. Asymmetric unit of **1** showing the labeling scheme used in the text and tables; hydrogen atoms have been excluded for clarity. Thermal ellipsoids are at the 50% probability level.

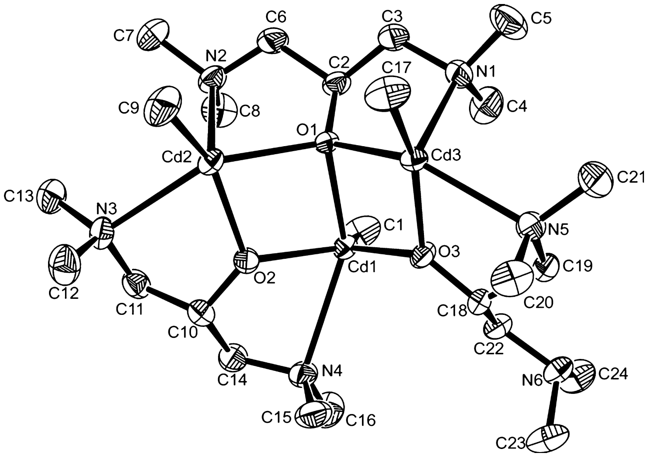

Figure 2. Asymmetric unit of **2** showing the labeling scheme used in the text and tables; hydrogen atoms have been excluded for clarity. Thermal ellipsoids are at the 50% probability level.

$$Me_2Cd + HOR \xrightarrow[\text{hexane}]{-HR} [MeCdOR']_x \qquad (1)$$

R	x
$CH_2CH_2NMe_2$ (**1**)	4
$CH(CH_2NMe_2)_2$ (**2**)	3
$C(CH_2NMe_2)_3$ (**3**)	2

We have also synthesized colorless Cd(tdmap)$_2$ (**5**) from Cd[N(SiMe$_3$)$_2$]$_2$, in 81% yield, by an amine elimination route:

$$Cd[N(SiMe_3)_2]_2 + 2HOC(CH_2NMe_2)_3 \xrightarrow{-2HN(SiMe_3)_2} Cd[OC(CH_2NMe_2)_3]_2 \qquad (2)$$

We were unable to prepare **5** from Me_2Cd and 2 equiv of alcohol, the reaction terminating with the formation of **3**.

All the compounds **1**−**5** are air- and moisture-sensitive and are soluble in common organic solvents.

Crystallography. The structures of **1**− **3** are shown in Figures 1, 2, and 4, respectively, with selected metrical data given in Tables 2− 4.

---

[39] Horley, G. A.; Mahon, M. F.; Molloy, K. C.; Haycock, P. W.; Myers, C. P. *Inorg. Chem.* **2002**, *41*, 5052–5058.

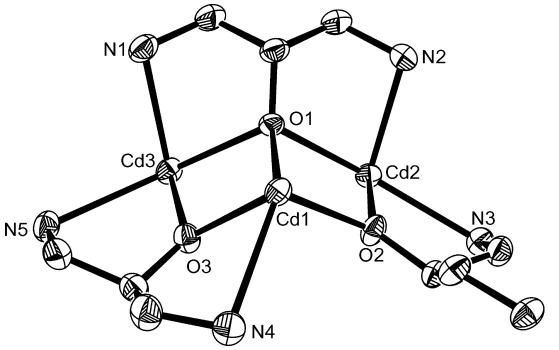

Figure 3. Core of **2** showing the angular nature of the fused Cd_2O_2 rings. Methyl groups and hydrogen atoms have been omitted for clarity.

Table 4. Selected Metrical Data for (**3**)[a]

bond lengths (Å)		bond angles (deg)	
Cd−C(1)	2.1449(13)	C(1)−Cd−O′	131.51(5)
Cd−O1′	2.2249(9)	C(1)−Cd−O	131.84(5)
Cd−O	2.2321(9)	C(1)−Cd−N(3)	123.22(5)
Cd−N(3)	2.4178(11)	O−Cd−O′	82.81(3)
		O−Cd−N(3)	76.26(3)
		O′−Cd−N(3)	93.92(3)
		Cd−O−Cd′	97.19(3)

[a] Symmetry transformation: 1 − *x*, −*y*, 1 − *z*.

MeCd(dmae) (**1**) adopts a tetrameric cubane structure typical of other $[RCdOR']_4$,[22,23] though the cube is rather distorted by the increase in cadmium coordination number to five, *via* chelation through the donor nitrogen. This has the effect of weakening four of the Cd−O bonds so that the cubane distorts toward a folded eight-membered ring:

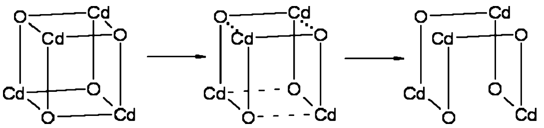

Thus, each metal has two short (*ca.* 2.2 Å) and one long (*ca.* 2.5 Å) Cd−O bonds. The four Cd−N bonds show little variation [2.516(3)−2.554(3) Å]. Each cadmium adopts a distorted trigonal bipyramidal geometry with a CdO_3NC coordination sphere, the axial positions being occupied by nitrogen and, not surprisingly, the oxygen of the long Cd−O bond. However, there is no discernible correlation between the strength of the N:$\rightarrow$Cd donation and the length of the long Cd−O bonds (though this might be expected) which implies that the overall cage geometry also plays a part in determining the pattern of bond lengths. All the dmae ligands behave as κ^2-*O,N* chelates while all the oxygen atoms adopt μ_3-bridging roles.

Incorporating an additional donor group in the ligand reduces the overall nuclearity of the complex to a trimer, as evidenced by $[MeCd(bdmap)]_3$ (**2**). The two terminal metals [Cd(2, 3)] are five-coordinated within a $CdCO_2N_2$ arrangement, while the central Cd(1), which is also five-coordinated, achieves this through a $CdCO_3N$ ligand set. In all three cases the geometry about the metal is heavily distorted toward a square-based pyramid if a τ-analysis is carried out.[40] For Cd(1), the nominal trigonal bipyramidal geometry has a single pair of candidates for the axial sites, with N(4) and O(1) generating the largest angle at cadmium [140.36(7)°]. For the other two metals the description is less clear. In both cases, two pairs of donors suggest themselves as possible axial ligands: C(9)−Cd(2)−O(2) 143.70(12), O(1)−Cd(2)−N(3) 139.23(7); C(17)−Cd(3)−O(7) 154.71(11), O(1)−Cd(3)−N(5) 149.35(7)°.

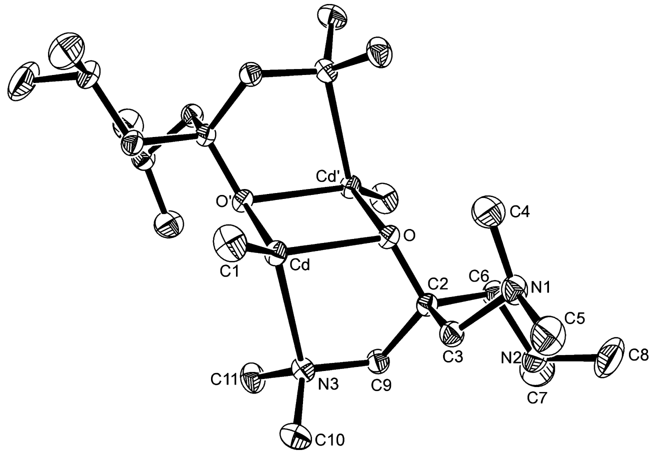

Figure 4. Asymmetric unit of **3** showing the labeling scheme used in the text and tables; hydrogen atoms have been excluded for clarity. Thermal ellipsoids are at the 50% probability level.

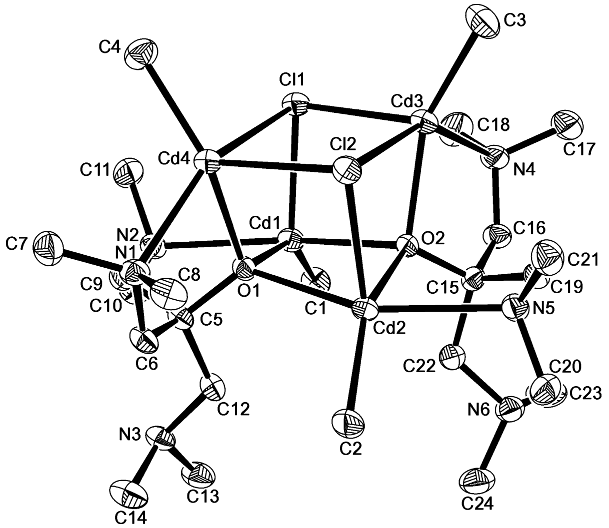

Figure 5. Asymmetric unit of **4** showing the labeling scheme used in the text and tables; hydrogen atoms have been excluded for clarity. Thermal ellipsoids are at the 50% probability level.

The two four-membered Cd_2O_2 rings are folded (Figure 3). Two of the bdmap ligands [based on O(1) and O(3)] span two metal centers in an κ^3-*O,N,N* manner as also seen in, for example, $SrCu_2(bdmap)_3(O_2CCF_3)_3$,[41] while that based on O(2) is an κ^2-*O,N* chelate; N(6) of this latter ligand remains uncomplexed. Both O(2) and O(3) adopt μ_2-bridging roles between cadmium centers while O(1) bridges all three metals in a μ_3-fashion. The longest Cd−O bond lengths are all associated with the μ_3-bridging center O(1). The chelating nitrogen centers fall into three groups. The shortest Cd−N bonds [Cd(2)−N(2) 2.489(3), Cd(3)−N(1) 2.460(3) Å] are associated with the longest Cd−O linkages, while the longest

---

(40) Addison, A. W.; Rao, T. N.; Reeddijk, J.; v Rijn, J.; Verschoor, G. C. *J. Chem. Soc., Dalton Trans.* **1984**, 1349.

(41) Breeze, S. R.; Wang, S.; Thompson, L. K. *Inorg. Chim. Acta* **1996**, *250*, 163.

Table 5. Selected Metrical Data for (**4**)

	Bond Lengths (Å)		
Cd(1)−O(1)	2.264(2)	Cd(3)−N(4)	2.468(3)
Cd(1)−O(2)	2.539(2)	Cd(4)−N(1)	2.424(3)
Cd(2)−O(1)	2.511(2)	Cd(1)−Cl(1)	2.5698(9)
Cd(2)−O(2)	2.275(2)	Cd(2)−Cl(2)	2.5910(9)
Cd(3)−O(2)	2.253(2)	Cd(3)−Cl(1)	2.6010(10)
Cd(4)−O(1)	2.269(2)	Cd(3)−Cl(2)	3.0274(9)
Cd(1)−N(2)	2.583(3)	Cd(4)−Cl(1)	3.2260(10)
Cd(2)−N(5)	2.554(3)	Cd(4)−Cl(2)	2.5864(9)
	Bond Angles (deg)		
O(1)−Cd(1)−O(2)	77.16(8)	O(2)−Cd(3)−N(4)	73.28(9)
O(1)−Cd(1)−N(2)	71.75(9)	O(2)−Cd(3)−Cl(1)	87.46(6)
O(1)−Cd(1)−Cl(1)	90.17(6)	O(2)−Cd(3)−Cl(2)	77.70(6)
O(2)−Cd(1)−N(2)	148.85(8)	N(4)−Cd(3)−Cl(1)	100.64(8)
O(2)−Cd(1)−Cl(1)	82.39(5)	N(4)−Cd(3)−Cl(2)	148.14(7)
Cl(1)−Cd(1)−N(2)	95.60(7)	Cl(1)−Cd(3)−Cl(2)	90.82(3)
O(1)−Cd(2)−O(2)	77.56(8)	O(1)−Cd(4)−N(1)	73.67(9)
O(1)−Cd(2)−N(5)	149.58(8)	O(1)−Cd(4)−Cl(1)	75.00(6)
O(1)−Cd(2)−Cl(2)	81.13(5)	O(1)−Cd(4)−Cl(2)	85.97(6)
O(2)−Cd(2)−N(5)	72.10(9)	N(1)−Cd(4)−Cl(1)	146.72(7)
O(2)−Cd(2)−Cl(2)	87.30(6)	N(1)−Cd(4)−Cl(2)	101.91(7)
N(5)−Cd(2)−Cl(2)	95.18(7)	Cl(1)−Cd(4)−Cl(2)	86.77(3)

Cd−N interactions [Cd(1)−N(4) 2.686(2), Cd(2)-N3) 2.659(3) Å] support the strongest Cd−O bonds involving O(2). N(5), which is part of the κ^2-*O,N* chelating bdmap, has an intermediate Cd−N bond [Cd(3)−N(5) 2.536(2) Å].

The tris-amino ligand tdmap reduces the nuclearity of the cadmium cluster still further to that of the dimer [MeCd(tdmap)]$_2$ (**3**), which is iso-structural with its zinc analogue (Figure 4).[42] Each cadmium is now tetrahedral, with Cd−O and Cd−N bonds which are at the short end of the respective ranges shown by **1** and **2**. The central Cd$_2$O$_2$ unit is rhombohedral, with a wider angle at the metal [O−Cd−O′ 131.51(5)°] than at the μ_2-oxygen [Cd−O−Cd′ 97.19(3)°]. The tdmap ligands behave in an κ^2-*O,N* chelating mode, as in **1**, with two potentially coordinating amine functionalities remaining passive. Thus, the dimeric nature of **3** is not due to coordination saturation of cadmium by the ligand, which would remove the need for additional O:$\rightarrow$Cd interactions, but must be a combination of the single donor and the overall ligand bulk, which is at least as sterically demanding as a *t*-butyl group.

Structures **1**−**3** can be viewed as a progression, in which a pair of vertices, that is, a CdO moiety, are sequentially removed from a cube:

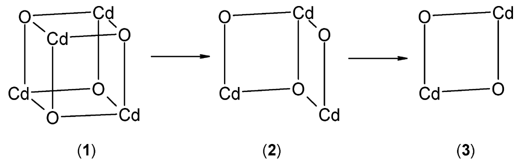

Also obtained serendipitously from the sample batch of **3** was a crystal of Me$_4$Cd$_4$(tdmap)$_2$Cl$_2$ (**4**) which appears unrepresentative of the batch as a whole and which we assume has arisen from traces of Htdmap.HCl in the ligand. The structure of **4** (Figure 5; Table 5) is a Cd$_4$O$_2$Cl$_2$ heterocubane. It is related to the cubane **1** with two chlorine atoms replacing two of the oxygens of the alcohol ligands in **1** and can be viewed as an assembly between two MeCd(tdmap) and two MeCdCl moieties. In each tdmap ligand two nitrogens chelate to a metal [N(1), N(2); N(4), N(5)] while two [N(3) and N(6)] remain free. Each cadmium retains the five-coordinate distorted trigonal bipyramidal geometry present in **1**, though in **4** there are distinct metal coordination spheres: CdCNCl$_2$O [Cd(3, 4)] and CdCNClO$_2$ [Cd(1, 2)]. Like **1**, the cubane distorts to a folded eight-membered ring as a result of two long Cd−O [Cd(1)−O(2) 2.539(2), Cd(2)−O(1) 2.511(2) Å] and two long Cd−Cl [Cd(3)−Cl(2) 3.0274(9), Cd(4)−Cl(1) 3.2260(10) Å] interactions. For comparison, short Cd−O and Cd−Cl bonds within the molecule are in the ranges 2.264(2)−2.275(2) and 2.5698(9)−2.6010(1) Å, respectively.

Table 6. Selected Metrical Data for (**5**)[a]

	Bond Lengths (Å)		
Cd(1)-O(1.	2.250(4)	Cd(2)−O(1)	2.254(2)
Cd(1)−O(2)	2.259(3)	Cd(2)−O(2)	2.218(4)
Cd(1)−O(4)	2.123(3)	Cd(2)−O(3)	2.140(3)
Cd(1)−N(1)	2.683(4)	Cd(2)−N(3)	2.457(4)
Cd(1)−N(5)	2.454(4)	Cd(2)−N(7)	2.558(3)
Cd(1)−N(10)	2.537(4)	Cd(2)−N(4)	2.643(3)
	Bond Angles (deg)		
O(1)−Cd(1)−O(2)	74.48(10)	O(2)−Cd(1)−N(10)	98.36(11)
O(1)−Cd(1)−O(4)	126.66(12)	O(4)−Cd(1)−N(1)	80.68(12)
O(1)−Cd(1)−N(1)	69.68(10)	O(4)−Cd(1)−N(5)	89.84(13)
O(1)−Cd(1)−N(5)	138.97(10)	O(4)−Cd(1)−N(10)	73.68(11)
O(1)−Cd(1)−N(10)	103.23(10)	N(1)−Cd(1)−N(5)	103.68(12)
O(2)−Cd(1)−O(4)	158.29(14)	N(1)−Cd(1)−N(10)	141.09(11)
O(2)−Cd(1)−N(1)	115.11(11)	N(5)−Cd(1)−N(10)	104.99(12)
O(2)−Cd(1)−N(5)	72.45(11)		
Cd(1)−O(1)−Cd(2)	104.42(13)	Cd(2)−O(2)−Cd(1)	105.32(13)

[a] Bond angles about Cd(1) only are given for conciseness.

The structure of Cd(tdmap)$_2$ (**5**) is shown in Figure 6, with selected metrical data in Table 6. The molecule is dimeric with a central Cd$_2$O$_2$ core (as in **3**) but lacking any crystallographic symmetry. In contrast to **3**, however, the enhanced Lewis acidity at cadmium resulting from the presence of two electronegative alcohol groups renders each metal six-coordinated with a *mer*-CdN$_3$O$_3$ coordination sphere, albeit that the octahedron is severely distorted. Within the central Cd$_2$O$_2$ core, one bond [Cd(2)−O(2)] is markedly shorter [2.218(4) Å] than the other three [2.250(4), 2.254(2), 2.259(3) Å] for no apparent reason. In addition, the angles at oxygen [104.42(13)°, 105.32(13)°] are wider than in **3** [97.19(3)°] to which it is most closely related structurally, as a result of a requirement for the ligand to chelate both metals by the amine groups, rather than only one. All six Cd−N bonds are similar [2.445(4)−2.683(4) Å]. The tdmap ligands are non-equivalent and fall into two pairs. The two μ_2 ligands which bridge the metals [based on O(1), O(2)] are κ^3 by virtue of also chelating to the two metals through the amine groups [N(1), N(3), N(4), N(5)]. In this respect these two ligands behave in a similar manner to the bdmap in **2**, leaving only one NMe$_2$ group on each of these ligands [N(2), N(6)] uncoordinated. In contrast, the two non-bridging tdmap ligands [based on O(3), O(4)] are κ^2-*O,N via* chelation, with two uncomplexed NMe$_2$ functionalities, as is seen in **3**.

NMR Spectroscopy. The NMR spectra of **1** at room temperature show a single resonance for ^{113}Cd (−301 ppm) and

---

(42) Johnson, A. L.; Hollingsworth, N.; Molloy, K. C.; Köhn, G., submitted for publication.

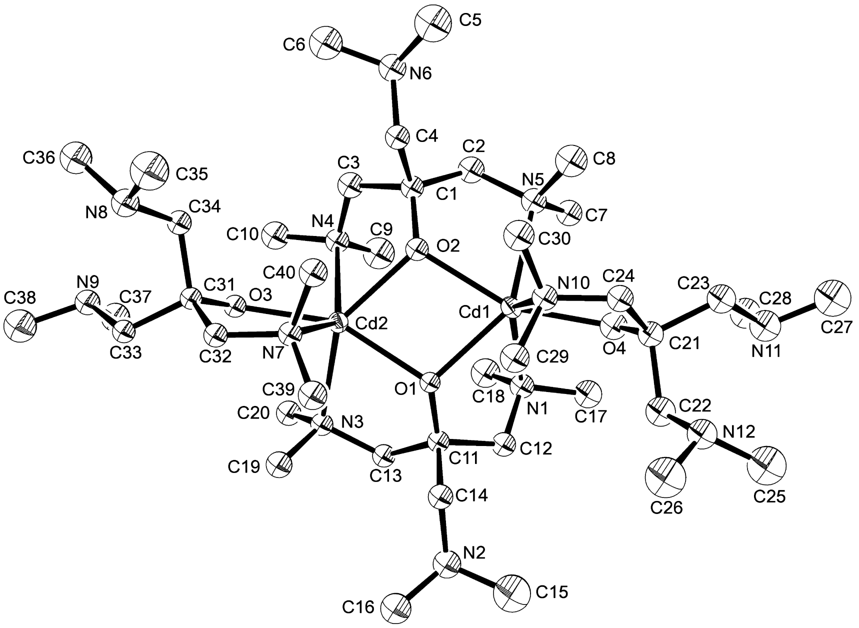

Figure 6. Asymmetric unit of **5** showing the labeling scheme used in the text and tables; hydrogen atoms have been excluded for clarity. Thermal ellipsoids are at the 50% probability level.

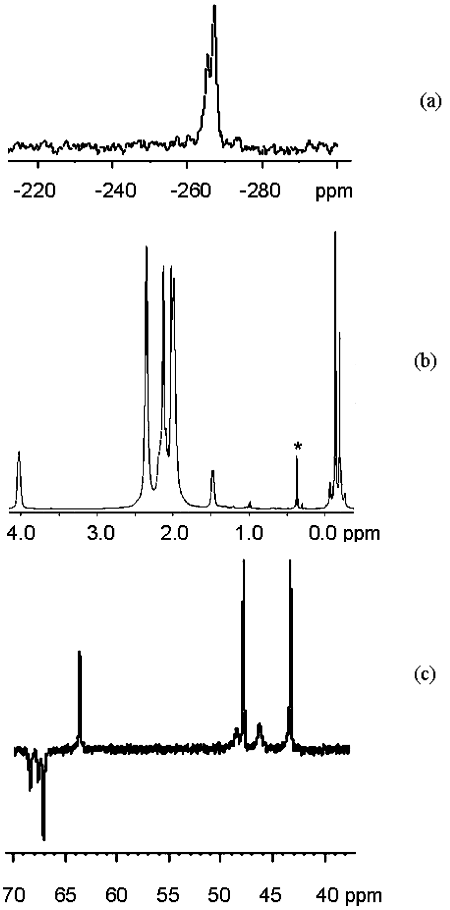

Figure 7. NMR spectra of **2** at 188 K: (a) ^{113}Cd, (b)^{1}H (impurity peak marked with *), and (c) 135 DEPT ^{13}C.

its associated methyl group at -0.42 ppm (^{1}H) and -18.3 ppm (^{13}C), the methyl signal showing ^{1}J and ^{2}J couplings to the metal (^{13}C: 1019, 1064; ^{1}H: 72.2, 77.7 Hz, for couplings to ^{111}Cd and ^{113}Cd, respectively). These coupling are about twice the magnitude of those seen in Me_2Cd (^{1}H: 50.0, unresolved; ^{13}C: 536, 512 Hz).[43] The ^{1}H and ^{13}C NMR also show a single environment for the ligand, with the only evidence for the different aminoalcohol environments seen in the crystallography being a broadening of the multiplet due to the OCH_2 protons at about 4 ppm. These spectra do not change in any significant way down to 188 K, the limit imposed by the freezing point of the solvent (toluene).

For **2**, the asymmetry in the structure is also not evident in the room temperature spectra, with only a single environment evident for cadmium (-279 ppm), the bound methyl group, and the aminoalcohol ligand. This is, perhaps, not surprising as far as the MeCd environments go, as each of the three metals is five-coordinated with similar (either $CdCO_2N_2$ or $CdCO_3N$) coordination spheres. What is not evident at room temperature, however, is any distinction between the two κ^3, μ_2 ligands and the κ^2 ligand which leaves one CH_2NMe_2 group uncoordinated. Clearly there is some fluxionality of the ligands at this temperature. The $^{1,2}J$ couplings to the cadmium [$^{2}J(^{111,113}\mathrm{CdH}) = 71.0, 73.8$, $^{1}J(^{111,113}\mathrm{CdH}) = 1000, 1043$ Hz] are similar to those in **1** which also has trigonal bipyramidal geometry about the metal. The ^{1}H NMR splittings of the ligand proton signals can be interpreted in terms of the following equivalences:

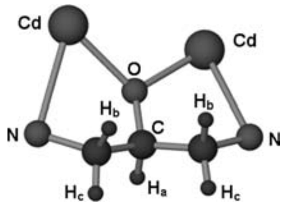

There are different chemical shifts for the inner (H_b) and outer (H_c) pair of methylene hydrogens, which couple to each

---

(43) Almond, M. J.; Beer, M. P.; Drew, M. G. B.; Rice, D. A. *Organometallics* **1991**, *10*, 2072.

other with $^2J = 11.5$ Hz. Both then couple with the methine H_a with $^3J = 9.7$ (H_b), 3.5 (H_c) Hz, the assignments being made on the basis of the dihedral angles $H_{b,c}{-}CCH_a$, (which are ca. 165°, 109°, respectively, from the structural data). The triplet of triplets observed for H_a ($^3J = 9.7$, 3.5 Hz) is consistent with this interpretation.

As the sample of **2** is cooled to 188 K the NMR spectra change to become consistent with the solid-state structure (Figure 7). At this temperature, two ^{113}Cd NMR signals are visible in a 2:1 ratio (−265, −267 ppm) consistent with the two terminal and one central metal environment, but all of which are five-coordinated (Figure 7a). In the ^{1}H NMR, the singlet at room temperature due to $CdCH_3$ also splits into two resonances at 198 K (−0.14, −0.19 ppm; 2:1), both signals showing coupling to cadmium, albeit that splitting to the two cadmium isotopes remained unresolved [J(CdH) = 71.5, 81.8 Hz] (Figure 7b). However, the corresponding ^{13}C NMR signal remains a singlet, though somewhat broader, at 188 K. The regions in both spectra due to the aminoalcohol ligand are complex but can be reconciled with the crystal structure in a general way. Thus, in the ^{1}H NMR spectrum there are four singlets due to the NMe_2 groups which divide into sets of four, four, two, and two methyl groups (δ = 2.36, 2.13, 2.01, 1.97 ppm) based on integration (2:2:1:1; Figure 7b), a pattern replicated in the ^{13}C NMR spectrum with two sharp equal intensity signals (δ = 43.0, 47.7 ppm) along with two broad resonances (δ = 46.0, 48.4 ppm) of half the area (Figure 7c). The two sharp signals we have assigned to the eight methyl groups of the two κ^3, μ_2 ligands, though we cannot be certain as to exactly how these are apportioned. The remaining, broader, signals are suggestive of some residual fluxionality, which we assign to the NMe_2 group coordinated to the central cadmium and the uncoordinated NMe_2 group [N(4) and N(6) in Figure 2], which are plausibly still exchanging roles even at low temperature. While the three CH units remain indistinguishable (δ = 4.03 broad, 63.9 ppm for ^{1}H and ^{13}C signals, respectively), the methylene groups are not. In the ^{13}C NMR spectrum, there are three CH_2 environments (δ = 68.9, 68.0, 67.5 ppm) which integration suggests are in the approximate ratio 2:1:3. Five of these carbon environments correlate with ^{1}H multiplets which lie under the NMe_2 singlets at between 2.50 and 1.70 ppm, while the unique CH_2 is associated with the CH_2 doublet at δ = 1.48 ppm [J(HH) = 8.9] which it seems reasonable to assign to the one uncoordinated CH_2NMe_2. Unexpectedly, the ^{13}C NMR shift for the methine carbon is more shielded (δ = 63.9 ppm) than the those of the NCH_2 groups, though this appears to also be the case in, for example, $Zn_4(OAc)_6(bdmap)_2$.[44]

The signals in the room temperature NMR spectra for **3** in $CDCl_3$ are the sharpest of all three compounds studied. The ^{113}Cd NMR signal comes at the most downfield shift (−228 ppm) which appears more diagnostic of the lower metal coordination number in this compound than the couplings inherent in the $CdCH_3$ moiety [$^2J(^{111,113}$CdH) = 73.6 Hz, unresolved; $^1J(^{111,113}$CdC) = 960, 1005 Hz] which are largely unchanged from the data for **1** and **2**, both of which contain more highly coordinated metal centers. Presumably, any redistribution in electron density arising from the higher coordination numbers in **1** and **2** impacts on the bonds to the aminoalcohol rather than the methyl groups. There is no discrimination between chelating and free CH_2NMe_2 functionalities at room temperature in either ^{1}H or ^{13}C NMR spectra consistent with a fluxional process in operation.

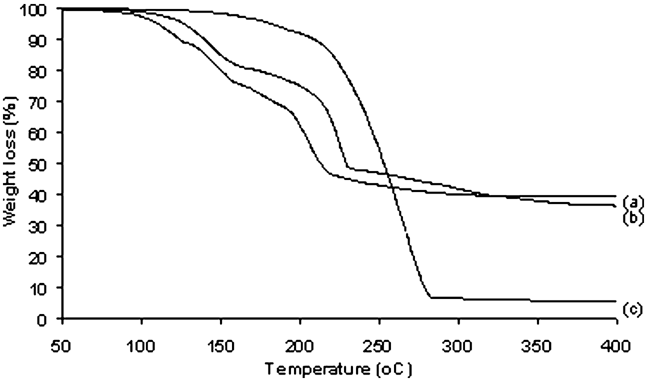

Figure 8. TGA of (a) **3**, (b) **6** and (c) [MeZn(tdmap)]$_2$.[42]

At lower temperatures, however, the spectra (in toluene) are more complex. The CH_3 singlet in the ^{1}H NMR at room temperature is broad to the extent that coupling to cadmium is not observed. This signal continues to broaden in the range 278 > T > 238 K, but at 218 K two relatively sharp signals appear, one [δ −0.35 ppm, $^2J(^{111,\ 113}$CdH) ~ 73 Hz, unresolved] due to **3** along with a second signal of double the intensity [δ −0.64 ppm, $^2J(^{111,\ 113}$CdH) ~ 40 Hz, unresolved] which we assign to Me_2Cd. The ^{113}Cd NMR spectra are consistent with this interpretation. At room temperature (in toluene) we see no signal, but as the temperature is lowered to 258 K two signals of approximately equal intensity appear which are sharp at 218 K: one at −211 ppm due to **3** (cf. −228 ppm at room temperature in $CDCl_3$), and a second at −6 ppm which is in the region expected for Me_2Cd (δ = 0 ppm at room temperature). Such spectra suggest the following equilibrium is operating:

$$\underset{(3)}{2\mathrm{MeCd(tdmap)}} \rightleftarrows \mathrm{Me_2Cd} + \underset{(5)}{\mathrm{Cd(tdmap)_2}} \qquad (3)$$

We have no evidence for the presence of $Cd(tdmap)_2$ from the ^{113}Cd NMR spectra of **3** at low temperatures but suggest that this species could have frozen out of solution at 218 K. The above equilibrium also implies that crystals of **3** are obtained from hexane because of its lack of solubility, which causes the above equilibrium to displace to the left.

In the light of the above comments, we have synthesiszed and recorded the NMR data for $Cd(tdmap)_2$ (**5**) for comparison. The room temperature ^{1}H NMR shows the signals for the NCH_2 and NCH_3 protons coincide to a broad singlet, but at 278 K these resolve themselves into two signals of appropriate intensities (2.43, 2.36 ppm); the room temperature HMQC spectrum of **5** also correlates the ^{1}H NMR "singlet" with the two quite distinct ^{13}C NMR resonances (OCH_2 69.4; NCH_3 49.8 ppm). At room temperature the ^{113}Cd NMR of **5** is a single peak at −453 ppm, which is the position required to average with Me_2Cd (−6 ppm) to give

---

[44] Demsar, A.; Kosmrlj, J.; Petricek, S. *J. Am. Chem. Soc.* **2002**, *124*, 3951.

the observed signal for MeCd(tdmap) (**3**) at −211 ppm. In addition, the signal due to **5** is negligible at 208 K, possibly because of it being frozen out of solution at this temperature as suggested from the low temperature NMR of **3**.

CVD Experiments. Thermogravimetric analysis (TGA) of **3** under a flowing N_2 stream (Figure 8a) shows that it is much less volatile than its zinc analogue, which sublimes cleanly at $T > \sim200$ °C (Figure 8c).

In contrast, **3** begins to decompose at $T > 100$ °C and decomposition is complete by 300 °C leaving a mass remaining (38.7%) consistent with CdO (38.9%). Decomposition seems to take place in three distinct stages, with two initial losses of about 11% (up to 130 and 160 °C, respectively). While we can only speculate as to the nature of these steps, 11% corresponds to loss of $EtNMe_2$, that is, loss of Me (from the metal) and CH_2NMe_2 from the ligand. That this step appears to take place twice is consistent with the presence of two CdMe functionalities and of free CH_2NMe_2 groups in both halves of the dimer.

Thin films of CdO have been deposited using $[MeCd(tdmap)]_2$ (**3**) under LPCVD conditions (ca. 0.1 mmHg). Both the precursor and substrate temperatures were 140 °C and the run time was 30 min. While the pecursor temperature did induce some *in situ* decomposition, lower temperatures did not generate sufficient carry over. Furthermore, while the substrate temperature is lower than that suggested by TGA for complete decomposition, higher temperatures resulted only in deposition on the walls of the hot wall reactor. That no carbon was observed in the final film suggests that the decomposition process is accentuated under vacuum. No ancillary oxygen source was used, making this the first true example of CdO deposition from an SSP.

A smooth, pale yellow film of approximate thickness 300 nm (Figure 9a) is formed, which energy-dispersive x-ray spectroscopy (EDXS) clearly shows contains cadmium and oxygen (Figure 9b). The XRD of this film (Figure 10) shows crystallinity despite the low deposition temperature and can be indexed to cubic CdO (PDF 75-1529); annealing at 500 °C for 3 h made negligible change to the appearance of the film. There is no preferred orientation to the film growth, in contrast to films grown from various adducts e.g. $Cd(hfac)_2(TMEDA)$, which show (200) texture.[17,18]

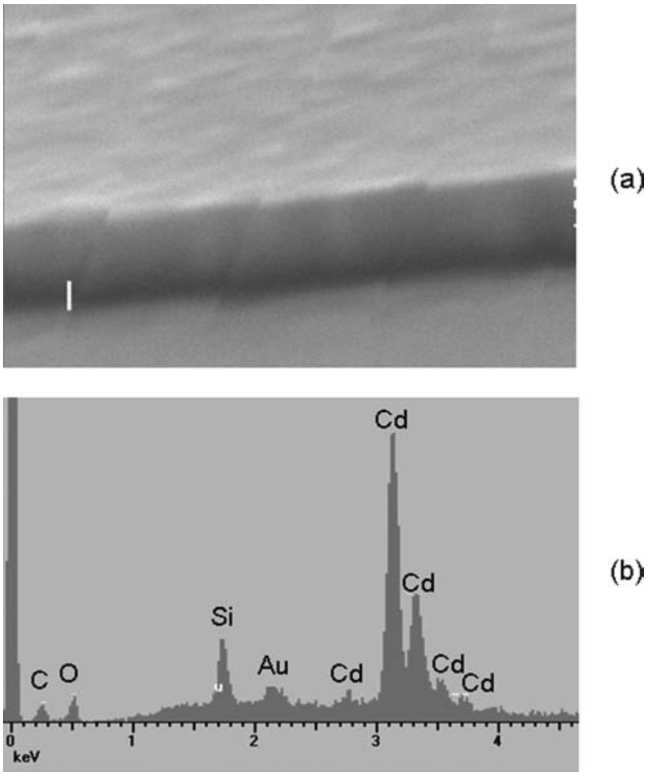

Figure 9. Film deposited from **3** under LPCVD conditions on a glass substrate (a) SEM (bar = 100 nm) and (b) EDXS (C, Au peaks are due to the sample preparation, Si results from the exposed glass substrate).

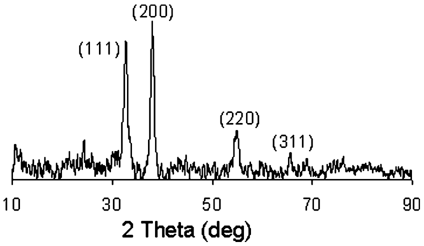

Figure 10. XRD of the film deposited from **3** as deposited. The film is indexed to cubic cadmium oxide (PDF 75-1529).

Mixed Cd/Zn system. In the light of the iso-structural nature of $[MeM(tdmap)]_2$ (M = Cd, Zn), we have attempted to prepare a mixed-metal system, $[(MeZn)(MeCd)(tdmap)_2]$ (**6**), to evaluate the possibility of depositing a mixed metal oxide by CVD. Incorporation of cadmium into a zinc oxide film is known to lower the bandgap of ZnO from 3.3 eV, while it also influences the green emission of zinc oxide phosphors. Initial attempts using a 50/50 mix of Et_2Zn and Me_2Cd with 2 equiv of Htdmap resulted only in a mixture of the homometallic dimers. However, when an equimolar mixture of Me_2Zn and Me_2Cd was reacted with Htdmap in the manner described for the preparation of **3**, a crystalline product was obtained which has a sharp melting point (145 °C), intermediate between that of **3** (105 °C) and its zinc analogue (173 °C).[42] The unit cell lengths for the crystal [$a = 10.1408(2)$, $b = 13.5406(3)$, $c = 11.7619(3)$ Å] are intermediate between those of **3** (Table 1) and $[MeZn(tdmap)]_2$ [9.90800(10), 13.7230(2), 11.64200(10) Å].[42] The structure solution, which is identical to that of **3** and $[MeZn(tdmap]_2$ in every respect, for example, space group, gives the lowest *R*-value for a 50:50 occupancy of the metal centers by Cd and Zn, though of itself this does not distinguish between disordered homometallic dimers or a mixed-metal species in which the two metals are disordered over the two sites.

^1H NMR of **6**, as with **3** and $[MeZn(tdmap)]_2$, gave broad peaks for the $OCCH_2$ protons on the tdmap ligand which appear at 2.51pmm, intermediate between the values seen for the homometallic species (2.46, 2.58 ppm for Cd, Zn, respectively). The singlet due to the $N(CH_3)_2$ hydrogens does, however, appears at the same position (2.30 ppm) as that seen for **3** and $[MeZn(tdmap)]_2$. There are two singlets corresponding to distinct $CdCH_3$, identified from its associated satellites (−0.37 ppm, $J = 746$ Hz, unresolved), and $ZnCH_3$ (−0.64 ppm; no satellites) centers, through perplexingly, while these integrate to the required six protons in total they are not in a 1:1 ratio (3.75:2.25 $CdCH_3/ZnCH_3$), despite the microanalytical data

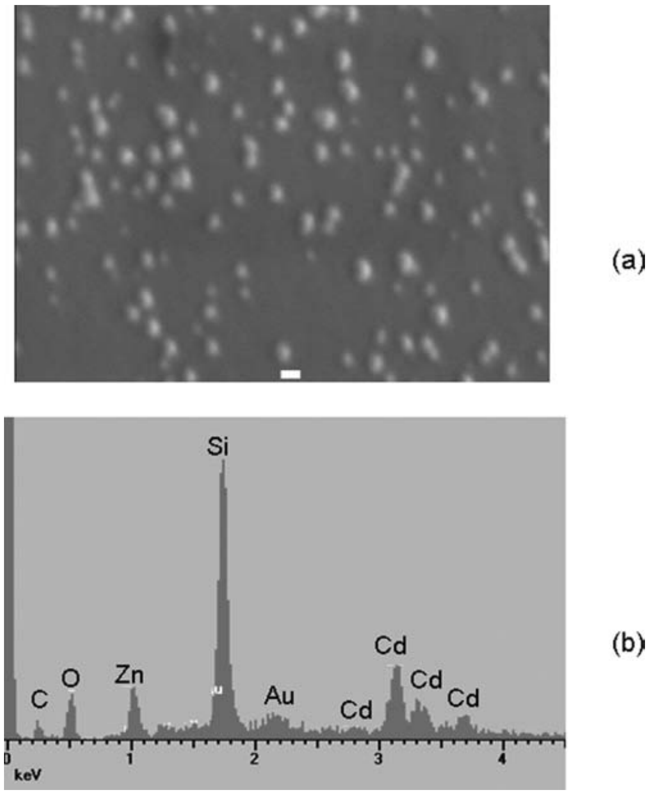

Figure 11. Film deposited from **6** under LPCVD conditions, (a) SEM (bar = 100 nm) and (b) EDXS of the film.

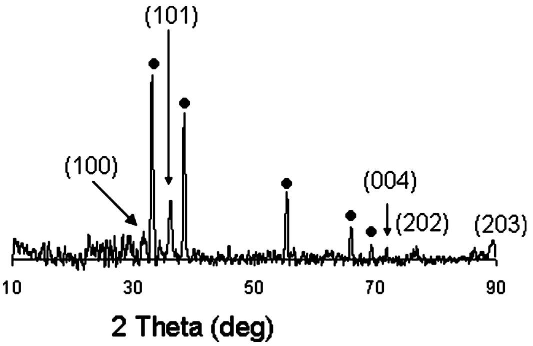

Figure 12. XRD of the film shown in Figure 10. Lines marked with ● correspond to cubic CdO (PDF 75-1529; see Figure 9), while those indexed correspond to hexagonal ZnO (PDF 80-0074).

which is consistent with equimolar amounts of the metals; this inequality in intensity is repeated in the ^{13}C NMR of the methylmetal signals. The ^{113}Cd NMR of a solution of this product shows two signals, one at −228 ppm corresponding to the Cd_2 species (**3**), along with a second signal at −254 ppm which we tentatively assign to the heterometallic dimer (MeZn)(MeCd)$(tdmap)_2$ (**6**). The ratio of the two signals, when normalized to allow for twice the number of cadmium centers in **3**, is about 1:1. That **6** equilibrates with the two homometallic dimers in solution is not unreasonable, given the facile Schlenk-type equilibrium observed for **3**.

Similarly, several species are seen in the mass spectrum of **6**. These include (MeZn)(MeCd)(tdmap), that is, (**6**-tdmap), at *m/z* 410.0717 (calcd 410.0708), (**3**-tdmap) at 460.0467 (calcd 460.0451) and $(MeZn)_2$(tdmap) at 360.0896 (calcd 360.0966), though other fragments at higher mass, as yet unidentified, are also visible.

In summary, we have synthesized a mixed-metal species which, *at least in part,* seems to contain both metals within the same dimeric assembly, though we cannot rule out that this co-exists with a mixture of homometallic dimers.

Despite the uncertainty in the nature of **6**, we have used it to deposit a film under identical LPCVD conditions to those described for **3**, above. The TGA of **6** is similar to that of **3** (Figure 8b) and quite unlike $[MeZn(tdmap)]_2$, with a residual mass (34.8%) at 350 °C consistent with ZnO + CdO (34.2%). Under the conditions of low substrate temperature used (140 °C) $[MeZn(tdmap)]_2$ does not generate a film, requiring temperatures about 500 °C to form ZnO.[42] The film produced by this mixed precursor **6** is different to that formed from **3** alone, showing spherical protrusions within a generally smooth film (Figure 11a) and, while pale yellow in appearance, darkens to orange on annealing at 500 °C in air over a 3 h period. For comparison, the CdO film remains pale yellow on annealing while a ZnO film darkens to brown under the same conditions.[42] The film is estimated to be about 200 nm in thickness. The EDXS of this film shows the presence of both metals, and, while the XRD pattern is dominated by lines from cubic CdO (PDF 75-1529), diffraction lines due to hexagonal ZnO (PDF 80-0074) are clearly visible, particularly the dominant (101) line of the randomly oriented material (Figure 12).

Conclusions

The nuclearity of MeCdOR clusters can be controlled using chelating aminoalcohols. Using only one chelating group (dmae), the ubiquitous tetrameric heterocubane structure is retained, albeit with an expansion in the coordination number at the metal to five. The bis-chelating ligand bdmap generates a trimer, while the tris-chelate tdmap affords a dimer. In this latter case, only one amine coordinates to cadmium so the structure adopted appears to be controlled by both the functionality inherent in the ligand and its steric bulk.

$[MeCd(tdmap)]_2$ can act as a true SSP for the deposition of CdO films at low temperatures (140 °C) under LPCVD conditions. In addition, a precursor containing, at least in part, (MeCd)(MeZn)$(tdmap)_2$, affords a film containing CdO with spherical particles of ZnO embedded, under similarly low temperature conditions.

Acknowledgment. We thank the EPSRC for a doctoral training award (to N.H.) and Mr H. R. Perrot (University of Bath) for help with the SEM and EDXS analyses of the thin films. Dr. A. Lubben (University of Bath) is thanked for help with recording the mass spectra, and SAFC Hi-tech are thanked for a gift of Me_2Cd.

Supporting Information Available: Crystallographic data for the structural analysis (in CIF format). This material is available free of charge via the Internet at http://pubs.acs.org. These data have also been deposited with the Cambridge Crystallographic Data Center, CCDC nos. 688193 (**3**), 688194 (**2**), 688195 (**1**), 688196 (**4**), and 688197 (**5**). Copies of this information may be obtained from the Director, CCDC, 12 Union Road, Cambridge, CB21EZ, UK (Fax: +44−1233−336033; e-mail: deposit@ccdc.cam.ac.uk or www.ccdc.cam.ac.uk).

IC800897T